

Pulsed Sonoelectrochemical Synthesis of Size-Controlled Copper Nanoparticles Stabilized by Poly(*N*-vinylpyrrolidone)

Iris Haas, Sangaraju Shanmugam, and Aharon Gedanken*

Department of Chemistry and Kanbar Laboratory for Nanomaterials at the Bar-Ilan University Center for Advanced Materials and Nanotechnology, Bar-Ilan University, Ramat-Gan, 52900, Israel

Received: July 5, 2006

A novel sonoelectrochemical method for the size-controlled synthesis of spherical copper nanoparticles in an aqueous phase was developed. In this study, poly(*N*-vinylpyrrolidone) (PVP) was used as the stabilizer for the copper clusters. The copper nanoparticles were characterized by XRD, UV–vis, IR, DLS, TEM, and HRTEM. The PVP was found to greatly promote the formation rate of copper particles and to significantly reduce the copper deposition rate, thereby making monodispersed copper nanoparticles. We could control the particle size by adjusting various parameters such as current density, deposition, temperature, and sonic power, and improve the homogeneity of the copper particles. The results also showed that the transfer rate of PVP-stabilized copper clusters from the cathodic vicinity to the bulk solution played an important role in the preparation of the monodispersed nanoparticles.

Introduction

Particles with sizes less than 100 nanometers are characterized by an extremely large surface-to-volume ratio, and their properties are determined mainly by the behavior of their surface.¹ In powder metallurgy, nanoparticles save energy due to lower sintering temperatures and the higher densities that are achieved. The preparation of uniform metallic nanomaterials using conventional techniques is rather difficult. The creation and future utilization of such types of nanosize systems requires the development of new technological processes. The industrial production of metallic nanoparticles in solutions requires overcoming the problems associated with the presence of the precursor electrolytes at high concentrations. This usually leads to coagulation and agglomeration of the particles, as can be expected from the DLVO theory.² The coagulation is followed by rapid sedimentation, due to the large aggregate size and the inherent high density of the metallic particles, which prevents their use in many applications in which a nanometric size is required. For example, applications based on thin layers of nanoparticles, such as security printing, require a homogeneous film formation in which individual nanoparticles are dispersed. Another application is the use of metallic particles for immunodiagnostic systems, onto which molecules having a specific recognition capability are adsorbed. Obviously, such applications would require the stable dispersions of nanoparticles, without sedimentation or aggregation.

At present, most scientific reports on the stabilization of dispersions of nanoparticles are focused on very dilute dispersions, prepared at very low precursor concentrations, thus avoiding the above problems. However, to achieve the feasibility of the industrial production of various metallic nanoparticles, there is an obvious need for developing suitable methodologies, especially for particles prepared by innovative methods. The synthesis of nanosized noble metal particles has attracted considerable interest in various fields of chemistry, due to its novel physicochemical properties that differ significantly from

macroscopic metal phases and its potential applications in many areas such as optics, microelectronics, catalysis, mechanics, information storage, and energy conversion.³ The shape and size of nanoparticles greatly affect the properties of metals on the nanometer scale, and it is therefore critical to develop an effective method for the preparation of nanoparticles with well-controlled shapes and sizes.⁴

Electrochemistry has not been extensively employed as a means for preparing large numbers of metal nanoparticles,⁵ but electrochemical methods do have some advantages over chemical techniques in the synthesis of small metal particles. The advantages are the high purity of the products and the possibility of precise control over the particle size, which can be achieved by adjusting the current density or the applied potential.⁶ Sonochemistry is the result of acoustic cavitations (i.e., the formation, growth, and impulsive collapse of bubbles in a liquid). The collapse of such a bubble creates hot spots with a temperature at high as 5000 K, pressures up to 1000 atm, and cooling rates in excess of 10¹⁰ K/s. These conditions are responsible for a variety of chemical and physical effects (for example, the decomposition of water to H and OH radicals in aqueous solutions).⁷

The potential benefit of combining both sonochemistry with electrochemistry is being increasingly studied. Some of their beneficial effects include the acceleration of mass transport, cleaning and degassing of the electrode surface, and increased reaction rates.⁸ Recently, pulse sonoelectrochemical synthesis, which was first introduced by Reisse et al.,⁹ involving alternating sonic and electric pulses has been employed to obtain the shape-controlled synthesis of nanostructured materials. The sonoelectrochemical formation of nanoscale metal and semiconductor powders was accomplished by applying an electric current pulse to nucleate the electrodeposit, followed by a burst of ultrasonic energy that removes the particles from the sonotrode. Qiu et al. synthesized highly dispersed palladium nanoparticles by sonoelectrochemical methods with different shapes and sizes in the presence of cetyl trimethylammonium bromide.¹⁰ Zhu et al. synthesized silver nanoparticles by sonoelectrochemical

* Corresponding author. E-mail: gedanken@mail.biu.ac.il.

methods with poly(vinylpyrrolidone) as a stabilizing agent.¹¹ Several synthetic techniques have been employed in the preparation of copper nanoparticles, including reverse micelles,¹² the reduction of copper(II) acetate in water and 2-ethoxyethanol using hydrazine under reflux,¹³ the reduction of an aqueous copper chloride solution using NaBH_4 in the nonionic water-in-oil (w/o) microemulsions,¹⁴ sonochemical synthesis,¹⁵ the γ -radiolysis method,¹⁶ use of carbon nanotubes as a template,¹⁷ the electro-exploding wire process,¹⁸ chemical reduction of Cu^{2+} ions dissolved in the water core of a water-in-supercritical CO_2 microemulsion,¹⁹ photochemical,²⁰ metal vapor synthesis,²¹ microwave irradiation,²² and laser ablation.²³ Reisse et al. synthesized copper powders by a sonoelectrochemical method.⁹ In this article, we report on an easier and more convenient sonoelectrochemical method for preparing large amounts of well-dispersed copper nanoparticles in an aqueous medium in the presence of poly(*N*-vinylpyrrolidone) (PVP) and demonstrate that the particle size distribution may be further improved by adding nonionic surfactants of appropriate concentrations to the electrolyte. Thus, the novelty of this article is not in the technique (i.e., sonoelectrochemistry) but rather the stabilization of the copper by PVP. This stabilized solution enabled us to study the particle size of the copper as a function of various parameters. The polymer also dictates the morphology of the copper nanoparticle. The prepared copper nanoparticles were characterized by various techniques such as X-ray diffraction (XRD), UV-vis, particle size analyzer, TEM, and HRTEM. The particle sizes were controlled by varying the experimental conditions.

Experimental Section

Materials. $\text{CuSO}_4 \cdot 5\text{H}_2\text{O}$ was purchased from Aldrich and used as received. Poly(vinylpyrrolidone) (PVP 40; MW 40 000) was obtained from Aldrich. The sonoelectrochemical device employed in these experiments has been described elsewhere^{11,12,24} and is similar to the instrument used by Reisse et al.⁹ In brief, a titanium horn (Ultrasonic liquid processor VC-600, 20 kHz, Sonics & Materials) acts as both the cathode and the ultrasound emitter. The electroactive part of the sonoelectrode is the planar circular surface, with an area of 1.23 cm^2 , at the bottom of the horn. The immersed cylindrical part is covered by an isolating plastic jacket. This sonoelectrode produces a sonic pulse that is triggered immediately following a current pulse. Our pulse driver (General Valve) is used to control a potentiostat, and a second pulser (Wavetek function generator 164) controls the ultrasonic processor, which is adapted to work in the pulse mode.²⁵ The home-built potentiostat is operated in the constant current regime (without using a reference electrode). A platinum wire spiral (0.5-mm diameter and 15-cm long) is used as a counter electrode. In the experiment producing copper without a stabilizer, the cathodic current density pulses (at the ultrasonic horn) were 480 mA/cm^2 . The duration of the current pulse was 900 ms. The off time of the current pulse was 900 ms. The duration of the ultrasonic pulse was 600 ms. The off time of the ultrasonic pulse was 300 ms.

Sonoelectrochemical Synthesis of Copper. A control reaction conducted without a polymer was our first sonoelectrochemical experiment. The electrolyte in the experiment was identical to that used by Reisse et al.⁹ (i.e., an aqueous solution of copper(II) sulfate pentahydrate (0.16 mol/lit) and sulfuric acid (1.84 mol/lit)). The electrolyte volume was 60 mL. The copper deposition was carried out in the electrochemical cell for 30 min. We used a cell with a sintered glass separating the anode and the cathode. At the end of the reaction, the precipitate was

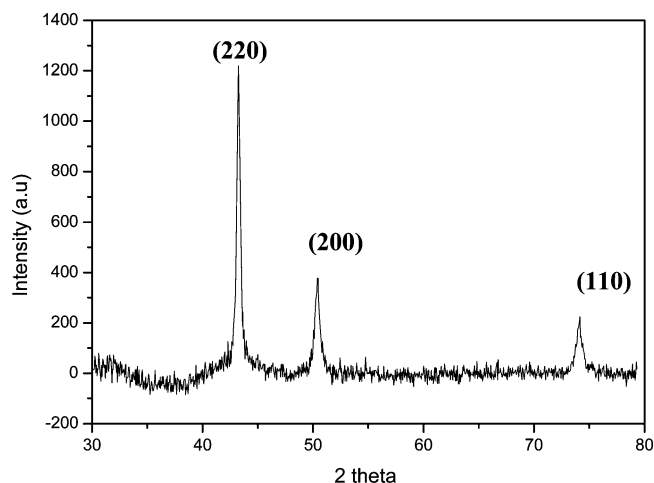


Figure 1. XRD pattern of a Cu nanoparticle.

washed repeatedly with distilled water and dried under vacuum overnight. The conditions included the duration of the current pulse, 250 ms, off time of the current pulse, 250 ms, and the duration of the ultrasonic pulse, 100 ms. The off time of the ultrasonic pulse was 150 ms.

Characterization. A Phillips EM-400T electron microscope operating at 80 kV was used for TEM and electron diffraction (ED), and a JEOL-2010 instrument with an accelerating voltage of 200 kV was used for HRTEM measurements. XRD of the powders was obtained using a Rigaku RU-200 B Rotaflex diffractometer operating in the Bragg configuration using $\text{Cu K}\alpha$ radiation. Data were collected with a counting rate of $0.25^\circ \text{ min}^{-1}$ and a sampling interval of 0.002° . The accelerating voltage was set at 50 kV with a 150 mA flux. Scatter and diffraction slits of 0.3 and 0.5 mm collection slits were used. The crystal size (coherence length) was estimated from the width of the diffraction peaks using the Debye-Scherrer relationship. The UV-visible absorption spectra were recorded on a Perkin-Elmer UV-visible spectrophotometer. The mean particle size and the particle size distribution were determined by dynamic light scattering (DLS). The suspension of particles in the aqueous solution was measured by a Coulter N-4 particle size analyzer. The measurements were conducted 10 min after the completion of the sonoelectrochemical process. The sample was examined in a quartz cuvette at room temperature without diluting the final solution.

Results and Discussion

Using PVP as a stabilizer in the sonoelectrochemical synthesis created a colloidal solution of copper. This solution was stable for 3 days, after which a red precipitate was detected at the bottom of the flask. The XRD patterns of the evaporated solution obtained after 30 min of sonoelectrochemical deposition are presented in Figure 1. All the diffraction peaks could be indexed to the face-centered cubic (fcc) phase of copper (JCPDS 04-836). No impurity diffraction peaks were detected, indicating the purity of the product obtained by this method. Figure 3 shows the absorbance spectrum of the dispersion copper nanoparticles after the sonoelectrochemical process. We observed an absorption band at 589 nm, which is due to the surface plasmon bands for the copper nanoparticles. It is well-known that the colloidal dispersion of metals exhibits an absorption band in the UV-vis regions due to collective excitations of the free electron (surface plasmon band). Liu et al. observed a similar absorbance value for copper nanoparticles prepared by chemical methods.²⁶

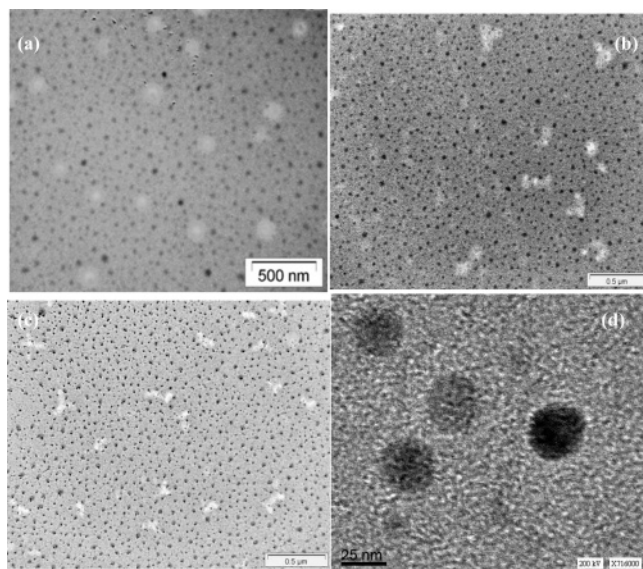


Figure 2. TEM image of copper nanoparticles: (a) 55, (b) 70, and (c) 100 mA/cm². (d) HRTEM image of image copper nanoparticles prepared with 55 mA/cm².

We base our interpretation of the stabilizing effect of PVP on results known for the Ag¹⁺–PVP composite structure.²⁷ The stabilizing mechanism of PVP in the electrochemical synthesis of silver particles is generally proposed on the basis of its structural features. PVP has the structure of a polyvinyl skeleton with polar groups. The polar group donates lone-pair electrons forming a coordinative interaction with copper ions, thus creating a complex compound. The polar groups are nitrogen and oxygen atoms. When PVP is used as a stabilizer for copper nanoparticles (eq 1 of Scheme 1), the first step is the formation of a coordinative bonding between PVP and copper ions, producing the Cu²⁺–PVP complex. The formed complex is present in the solution. When the current pulse is applied, the Cu²⁺ is reduced to Cu⁰ on the polymer (eq 2 of Scheme 1), preventing the agglomeration of the metallic nanoparticles. The one or two copper atoms bound to the polar group autocatalyze the further reduction of the copper ions, forming a particle of about 30 nm that contains about 1000 copper atoms. The IR spectrum of PVP exhibits peaks at 2868 and 2952 cm^{−1} assigned to the C–H stretching vibrations. The peak at 1665 cm^{−1}

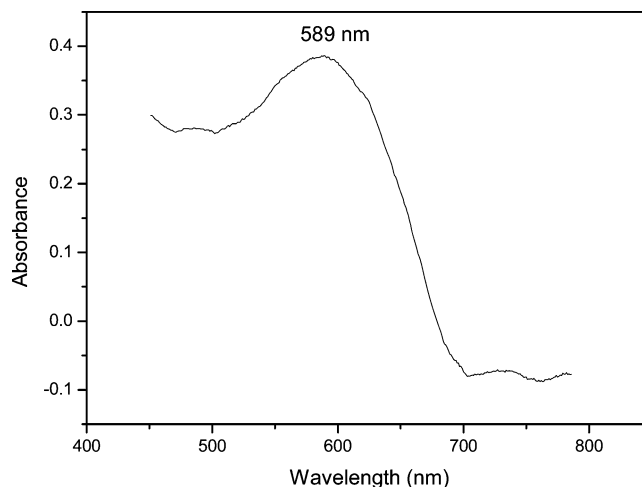


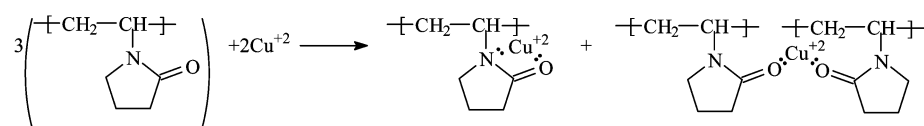
Figure 3. UV–visible absorption spectra of copper nanoparticles.

corresponds to the C=O vibrational mode of PVP (Figure 4a).²⁷ The IR spectrum of CuSO₄ shows a band at 1057 cm^{−1} (Figure 4b). In the CuSO₄–PVP complex, the band at 1057 cm^{−1} is shifted to 1073 cm^{−1}, indicating the interaction between the PVP and CuSO₄. A shift in the opposite direction is also revealed. When comparing the IR spectra of the PVP with that of the CuSO₄–PVP complex, the peak at 1665 cm^{−1} is red-shifted to 1650 cm^{−1} (Figure 4). The decrease in the wavenumber for C=O absorption may result from bond weakening via the partial donation of oxygen lone pair electrons of PVP to the vacant orbitals of the copper surface. The band at 1283 cm^{−1} is shifted to a higher wavenumber (1286 cm^{−1}) in CuSO₄–PVP, indicating the Cu ion interaction with C–N. These observations indicate that PVP coordinates with copper through the C–N and C=O groups.

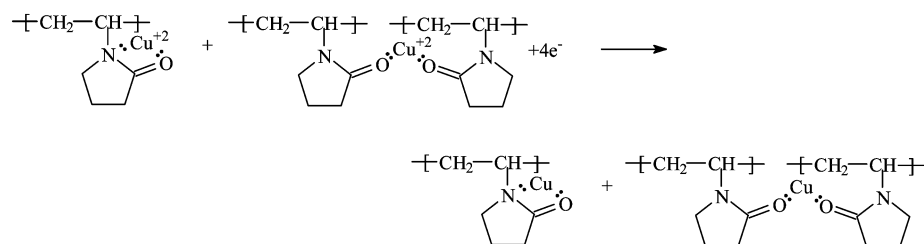
The morphology of the powder was found by dispersing the product on a copper grid coated with carbon and measuring its TEM. Figure 2 shows the TEM image of products obtained at different current densities for 30 min of sonoelectrochemical deposition. It can be seen from the TEM images that spherical and monodispersed particles are obtained. A partial white spherical background is observed in the TEM images, which we believe is an artifact of the microscope. A histogram of the size distribution of the particles is calculated by counting 200

SCHEME 1: Possible Bonding Framework for the Interaction between the Cu⁰ and the PVP

[Eq.1]



[Eq.2]



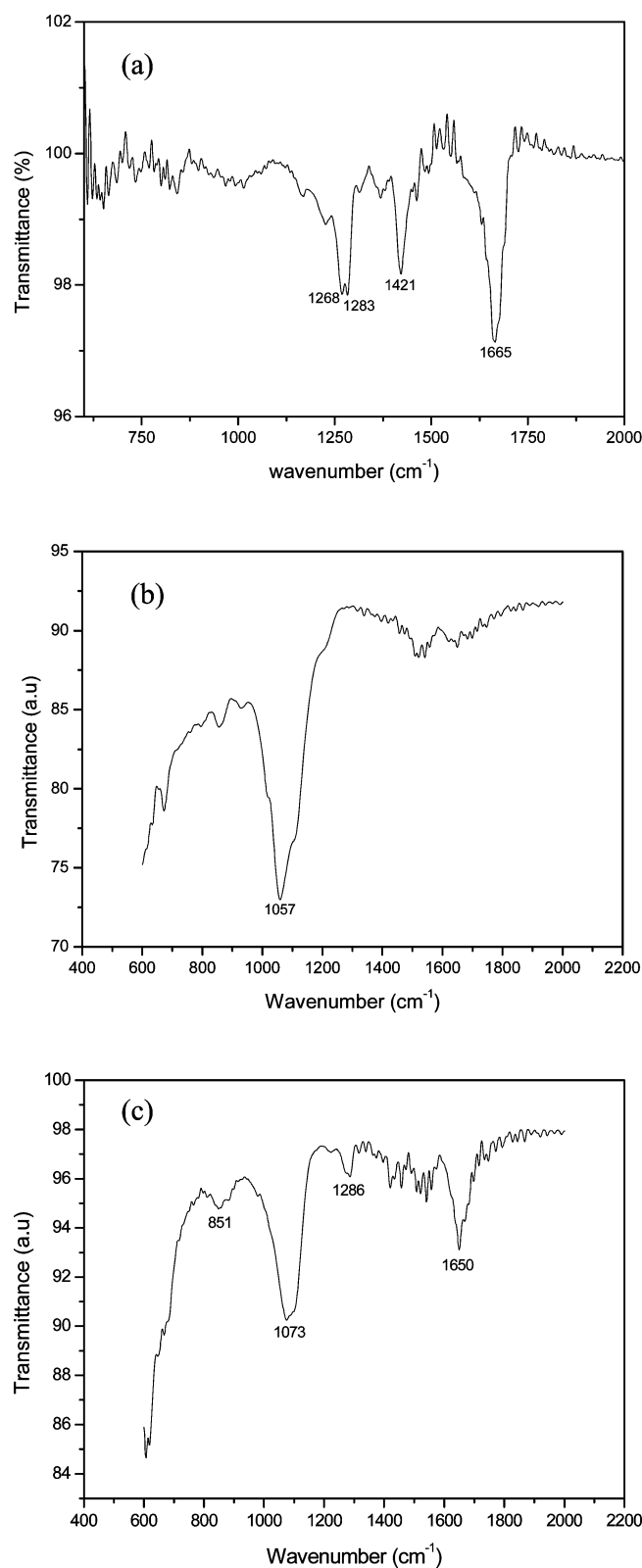


Figure 4. FTIR spectra of (a) PVP, (b) CuSO_4 , and (c) CuSO_4 -PVP.

particle sizes on the TEM grid. We found that the average particle size is around 29.0 ± 2.0 nm. Its size and distribution are also determined by DLS measurements. The scattering analysis also provides evidence of the narrow size distribution of the copper nanoparticles, as detected in the sonoelectrochemical experiments. The mean diameter of the copper nanoparticles was found to be 34 ± 4 nm, which is in good agreement with the results obtained from TEM.

TABLE 1: Effect of Various Deposition Parameters on Cu Particle Size

variable parameter	expt no.	sample conditions	particle size (nm)
current density (mA/cm^2)	1	55	29 ± 2
	2	70	24 ± 4
	3	100	10 ± 2
experiment duration (min)	4	10	23 ± 2
	5	30	29 ± 2
	6	60	38 ± 4
PVP concentration (%)	7	0.2	55 ± 10
	8	1	33 ± 2
	9	2	29 ± 2
temperature ($^\circ\text{C}$)	10	15	17 ± 3
	11	25	29 ± 2
	12	50	62 ± 5
sonic power (W)	13	35	29 ± 2
	14	50	29 ± 2
	15	76	29 ± 2

In addition, we have also carried out HRTEM measurements, which provided more information on the morphology and particle size of the product. Figure 2d depicts an example of such a particle. It should be noted that fringes are detected only in the left part of the particle, and the distance between the fringes, 0.208 nm, is in good agreement with the d value of the (111) plane of Cu^0 (0.208 nm according to JCPDS No. 04-836).

The formation of nanoparticles in sonoelectrochemistry is due to the massive nucleation caused by the relatively high current density electrodeposition pulse ($55\text{--}100 \text{ mA}/\text{cm}^2$), followed by the removal of the deposit from the electrode by the sonic pulse. The removal of the Cu from the electrode occurs before the next current pulse, thus preventing crystal growth. Finding the appropriate surfactant that yielded a stable colloidal solution consisting of nonaggregated particles enabled us to study the effect of the many experimental parameters on the particle size. To understand the formation of copper nanoparticles by the sonoelectrochemical method, we varied parameters such as electrodeposition time, current density, concentration of the stabilizer, temperature, and sonic power (Table 1).

We have attempted to find the Cu particle size dependence on the electric pulse width. However, the changes introduced in the pulse width were simultaneously accompanied by variations in the current. On the other hand, clear particle size dependence was observed for the current density variation. The current density was found to be an important parameter for controlling the size of the copper nanoparticles.²⁸ When we changed the current densities from 55, 70, and $100 \text{ mA}/\text{cm}^2$, the particle sizes changed (Figure 5). The particle size values obtained were 29 ± 2 , 24 ± 4 , and 10 ± 2 nm, respectively. Thus, the current densities dramatically affect the size of the copper nanoparticles. This behavior is explained as follows: For the low current density, the reduction rate of Cu^{2+} is slow and the number of nuclei is small, but the particle size is large. With an increase in the current, the enhanced reduction rates favor the generation of many more nuclei and the formation of smaller copper nanoparticles. In the present study, the range of the current is $55\text{--}100 \text{ mA}/\text{cm}^2$. The particle size is varied from 29 to 10 nm because the reduction rate of Cu^{2+} is much faster than the nucleation rate, and almost all the Cu^{2+} is reduced to atoms before the formation of the nuclei. The nucleation rate does not rise further, and the number of nuclei remains constant with increasing current. This observation is consistent with the literature.^{6,28}

The dependence of particle size on the experiment duration was probed by varying the deposition time from 10 min to 1 h. We observed that the particle size increased from 23 ± 2 to 38

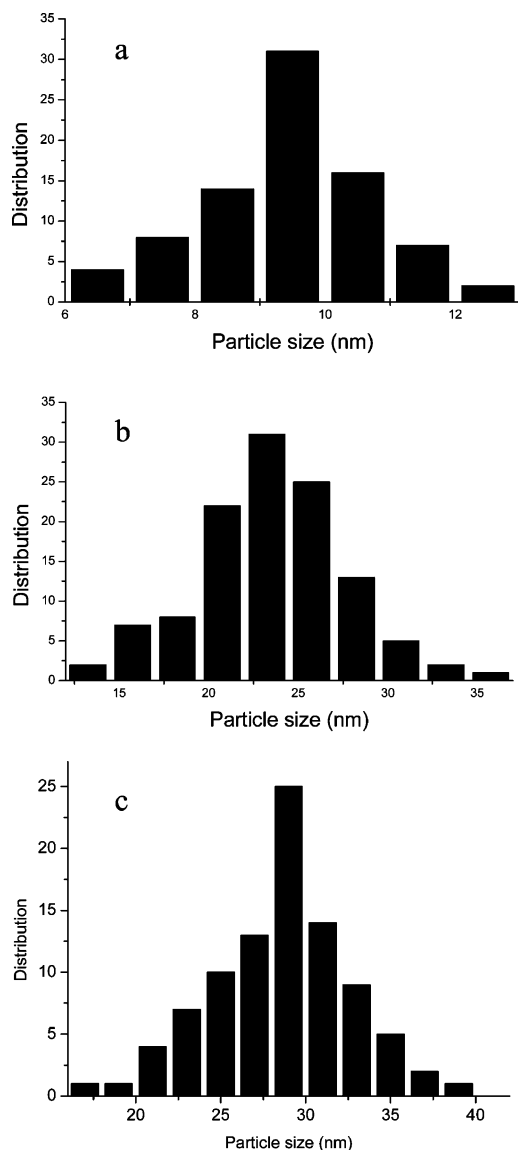


Figure 5. Particle size distributions for copper deposition at different current densities: (a) 100, (b) 70, and (c) 55 mA/cm².

± 4 nm. The explanation for this change in size is as follows: we carried out the reaction varying only the experiment duration and keeping all the other parameters the same, including the PVP concentration. The experiment's duration was varied from 10 to 30 min and to 60 min. An increase in the amount of metallic copper is clearly observed upon increasing the experiment's duration. The increase in the particle size is due to the higher amount of Cu⁰ that is obtained, and thus the PVP encases larger particles. Support for this pattern can be seen in the PVP concentration studies. Another explanation for the dependence of particle size on experiment duration is related to the copper nanoparticles acting as a suspensive electrode. Therefore, the deposition time changes the depletion of the copper ion concentration in the solution, and the particle size increases as the deposition time increases. Following the suspensive electrode model, which was proposed by Zaban et al.,²⁹ the initial thin copper layer is deposited on the sonotrode by the electric pulse. The following sonic pulse leads to the destruction of this layer on the cathode and the suspension of the copper nanoparticles. The deposited copper nanoparticle acts as a suspensive electrode. From that point on, two simultaneous processes occur. First, the sonoelectrode continues the electrodeposition of more copper particles. In the second process, the suspended particles are

moved in the solution by the sonic wave, hit the sonoelectrode, accept its potential, and travel back to the solution as a negative ion. These charged particles act as part of the cathode and can reduce more Cu²⁺ ions, enabling the electrodeposition of more metallic copper ion from the solution, leading to the further growth of the particle.

We have also synthesized sonoelectrochemically copper without a stabilizer and observed a highly agglomerated copper powder. This led us to study the effect of the concentration of the stabilizer on the particle size. The molar ratios of Cu(II)/PVP are 0.96:0.27, 0.96:0.56, and 0.96:1.1 for the 0.5, 1, and 2% solutions, respectively. When the concentration of PVP was 0.5% (wt), 55 ± 10 nm copper nanoparticles were measured. Well-dispersed copper nanoparticles were observed when the concentration of PVP was increased to 2% with an average particle size of 29 ± 2 nm. For the 2% (wt) PVP solution, there should be enough sites on the polymer to accommodate all the ions. However, a 0.5% (wt) solution cannot accommodate all of the Cu²⁺ ions, and therefore it may be possible to obtain broadly distributed copper nanoparticles. The size of the copper nanoparticles is larger when the PVP concentration is low (0.5%) because some Cu²⁺ ions are not coordinated to the polymer skeleton, and hence, their growth is not mediated by the polymer. In addition, the particles obtained with a 0.5% (wt) polymer concentration have a broader distribution of sizes than that of 1 and 2% (wt) PVP. These results are in accordance with the many studies demonstrating that an increase in the surfactant's concentration leads to the formation of smaller particles.^{11,27} In Table 1, we present the size dependence of the copper particles on the surfactant concentration.

We have also varied the temperature of the solution and studied the changes in particle size. The sizes obtained for reactions carried out at 15 and 25 °C were 17 ± 3 and 29 ± 2 nm, respectively. When we further increased the temperature to 50 °C, agglomerated (62 ± 5 nm) copper nanoparticles were obtained. Temperature can affect the crystal growth in several ways, all of them resulting in a smaller crystal size at lower temperatures. The simple explanation for this is that crystal growth is slower at lower temperatures. Another temperature effect might be related to the thermodynamic instability of very small nuclei below a certain critical size. This kinetic destabilization is more effective at lower temperatures. As the temperature increases, the supersaturation decreases, which will lead to a decrease in nucleation density, and hence, the particle size increases as the temperature increases.²⁴ These nuclei can redissolve, or may be thermodynamically stable, for long enough to grow larger than the critical size. This is a common mechanism to explain the decrease in colloid size with a decrease in temperature.³⁰ Another additional effect that might be operative here is the presence of the heterogeneous substrate (the electrode), which can exert an additional stabilizing influence on nuclei that would be subcritical in the absence of this surface.

We also studied the particle-size dependence on sonic power. The sonic power is responsible for the removal of the deposited particles from the electrode. When we increased the sonic intensity to 35 W, 29 ± 2 nm copper nanoparticles were obtained. A further increase in the sonic intensity does not show any change in the particle size. We explain these results as follows: certain intensity is required to remove efficiently all the deposited metallic copper from the electrode. Unless the reaction parameters are changed, the sonic intensity can no longer affect the particle size.

Conclusions

We described herein a pulsed sonoelectrochemical method for the synthesis of metallic copper nanoparticles in the presence of poly(vinylpyrrolidone) as a protecting agent. We observed monodispersed spherical copper nanoparticles with a diameter range of 25–60 nm. The particle size is controlled by varying reaction parameters such as duration of the experiment, current density, temperature, and sonic power. The current density plays an important role in controlling the size of the copper nanoparticles. We showed that the PVP is coordinated with copper through C–N and C=O bonds, evidenced by IR studies. This method can be extended to prepare other metals, bimetallic, core–shell nanoparticles by adopting suitable synthetic strategies.

Acknowledgment. This project was supported by the European Community Sixth Framework Program through a STREP grant to the SELECTNANO Consortium, Contract No. 516922.03/25/2005.

References and Notes

- (1) Henglein, A. *Chem. Rev.* **1989**, 89, 1861.
- (2) Cushing, B. L.; Kolesnichenko, V. L.; O'Connor, C. J. *Chem. Rev.* **2004**, 104, 3893.
- (3) (a) Sun, Y.; Xia, Y. *Science* **2002**, 298, 2176. (b) Yao, J. L.; Pan, G. P.; Xue, K. H.; Wu, D. Y.; Ren, B.; Sun, D. M.; Tang, J.; Xu, X.; Tian, Z. Q. *Pure Appl. Chem.* **2000**, 72, 221. (c) Hu, J. T.; Odom, T. W.; Lieber, C. M. *Acc. Chem. Res.* **1999**, 32, 435. (d) McConnell, W. P.; Novak, J. P.; Brousseau, L. C.; Fuierer, R. R.; Tenent, R. C.; Feldheim, D. L. *J. Phys. Chem. B* **2000**, 104, 8925. (e) Andres, P. R.; Bielefeld, J. D.; Henderson, J. I.; Janes, D. B.; Kolagunta, V. R.; Kubiak, C. P.; Mahoney, W. J.; Osifchin, R. G. *Science* **1996**, 273, 1960. (f) Andres, P. R.; Bein, T.; Dorogi, M.; Feng, S.; Henderson, J. I.; Kubiak, C. P.; Mahoney, W.; Osifchin, R. G.; Reifenberger, R. *Science* **1996**, 272, 1323. (g) Forster, S.; Antonietti, M. *Adv. Mater.* **1998**, 10, 195.
- (4) (a) Nie, S.; Emory, S. R. *Science* **1997**, 275, 1102. (b) Buffat, P.; Borel, J. P. *Phys. Rev. A* **1976**, 13, 3287. (c) Castro, T.; Reifenberger, R.; Choi, E.; Andres, P. R. *Phys. Rev. B* **1990**, 42, 8548. (d) Link, S.; El-Sayed, M. A. *J. Phys. Chem. B* **1999**, 103, 8410. (e) Petit, C.; Taleb, A.; Pileni, M. P. *J. Phys. Chem. B* **1999**, 103, 1805.
- (5) Zoval, J. V.; Stiger, R. M.; Biernacki, P. R.; Penner, R. M. *J. Phys. Chem.* **1996**, 100, 837.
- (6) Rodriguez-Sanchez, L.; Blanco, M. C.; Lopez-Quintela, M. A. *J. Phys. Chem. B* **2000**, 104, 9683.
- (7) (a) Suslick, K. S. The chemistry of ultrasound. From Yearbook of Science & the Future. Encyclopaedia Britannica: Chicago, 1994; pp 138–155. (b) Suslick, K. S. *Annu. Rev. Mater. Sci.* **1999**, 29, 295.
- (8) Mason, T. J.; Lorimer, J. P.; Walton, D. J. *Ultrasonics* **1990**, 28, 333.
- (9) (a) Reisse, J.; Caulier, T.; Deckerkheer, C.; Fabre, O.; Vandercammen, J.; Delplancke, J. L.; Winand, R. *Ultrason. Sonochem.* **1996**, 3, s147. (b) Durant, A.; Delplancke, J. L.; Winand, R.; Reisse, J. *Tetrahedron Lett.* **1995**, 36, 4257. (c) Reisse, J.; Francois, H.; Vandercammen, J.; Fabre, O.; Kirsch-de mesmaeker, A.; Maerschalk, C.; Delplancke, J. L. *Electrochim. Acta* **1994**, 39, 37.
- (10) Qiu, X. F.; Xu, J. Z.; Zhu, J. M.; Zhu, J. J.; Xu, S.; Chen, H. Y. *J. Mater. Res.* **2003**, 18, 1399.
- (11) Jiang, L. P.; Wang, A. N.; Zhao, Y.; Zhang, J. R.; Zhu, J. J. *Inorg. Chem. Commun.* **2004**, 7, 506.
- (12) Pileni, M. P.; Lisiecki, I. *Colloids Surf., A* **1993**, 80, 63.
- (13) Huang, H. H.; Yan, F. Q.; Kek, Y. M.; Chew, C. H.; Xu, G. Q.; Ji, W.; Oh, P. S.; Tang, S. H. *Langmuir* **1997**, 13, 172.
- (14) Qi, L. M.; Ma, J. M.; Shen, J. L. *J. Colloid Interface Sci.* **1997**, 186, 498.
- (15) Dhas, N. A.; Raj, C. P.; Gedanken, A. *Chem. Mater.* **1998**, 10, 1446.
- (16) Joshi, S. S.; Patil, S. F.; Iyer, V.; Mahumuni, S. *Nanostruct. Mater.* **1998**, 10, 1135.
- (17) Chen, P.; Wu, X.; Lin, J.; Tan, K. L. *J. Phys. Chem. B* **1999**, 103, 4559.
- (18) Tepper, F. *Int. J. Powder Metall.* **1999**, 35, 39.
- (19) Wai, C. M.; Ohde, H. J. *Chin. Inst. Chem. Eng.* **2001**, 32, 253.
- (20) Giuffrida, S.; Condorelli, G. G.; Costanzo, L. L.; Fragala, I. L.; Ventimiglia, G.; Vecchio, G. *Chem. Mater.* **2004**, 16, 1260.
- (21) Ponce, A. A.; Klabunde, K. J. *J. Mol. Catal. A: Chem.* **2005**, 225, 1.
- (22) (a) Zhu, H. T.; Zhang, C. Y.; Yin, Y. S. *J. Cryst. Growth* **2004**, 270, 722. (b) Zhu, H.; Zhang, C.; Yin, Y. *Nanotechnology* **2005**, 16, 3079.
- (23) Yeh, M. S.; Yang, Y. S.; Lee, Y. P.; Lee, H. F.; Yeh, Y. H.; Yeh, C. S. *J. Phys. Chem. B* **1999**, 103, 6851.
- (24) (a) Mastai, Y.; Polsky, R.; Koltypin, Y.; Gedanken, A.; Hodes, G. *J. Am. Chem. Soc.* **1999**, 121, 10047. (b) Zhu, J.; Liu, S.; Palchik, O.; Koltypin, Y.; Gedanken, A. *Langmuir* **2000**, 16, 6396. (c) Mohamed, M. B.; Wang, Z. L.; El-Sayed, M. A. *J. Phys. Chem. A* **1999**, 103, 10255.
- (25) Haas, I.; Gedanken, A. *Chem. Mater.* **2006**, 18, 1184.
- (26) (a) Wilcoxson, J. P.; Williamson, R. L.; Baughman, R. *J. Chem. Phys.* **1993**, 12, 9933. (b) Liu, C. M.; Guo, L.; Xu, H. B.; Wu, Z. Y.; Weber, J. *Microelectron. Eng.* **2003**, 66, 107.
- (27) Zhang, Z.; Zhao, B.; Hu, L. *J. Solid State Chem.* **1996**, 121, 105.
- (28) (a) Reetz, M. T.; Helbig, W. *J. Am. Chem. Soc.* **1994**, 116, 7401. (b) Zhu, J.; Aruna, S. T.; Koltypin, Y.; Gedanken, A. *Chem. Mater.* **2000**, 12, 143.
- (29) Socol, Y.; Abramson, O.; Gedanken, A.; Meshorer, Y.; Berenstein, L.; Zaban, A. *Langmuir* **2002**, 18, 4736.
- (30) Shedam, M. R.; Venkateswara Rao, A. *Mater. Chem. Phys.* **1998**, 52, 263.